Eur. Phys. J. D **11**, 449–456 (2000)

THE EUROPEAN PHYSICAL JOURNAL D

EDP Sciences

On the design of a Nd^{3+} doped silica fiber-laser using a cholesteric liquid crystal mirror

C. Li, J. Boyaval, M. Warenghem, and P. Carette[a]

Laboratoire de Physico-Chimie des Interfaces et Applications, Université d'Artois, Faculté des Sciences Jean Perrin, rue Jean Souvraz, S.P. 18, 62307 Lens Cedex, France

Received 21 October 1999 and Received in final form 7 February 2000

Abstract. We report operation of a Nd^{3+}-doped fiber-laser using a cholesteric liquid crystal acting as a narrow band reflector. The aim of this work is to apply to a fiber-laser the particular optical properties of an helical structure, whatever is the medium exhibiting this structure, either a liquid crystal or either any other material. The advantage of the use of these mediums in the design of fiber-lasers is that they can favourably take the place, in an easy and compact way, of several optical elements such as a polarizer and a quarter-wave plate at one and the same time. This technology promises to design rugged compact low cost tunable coherent sources the lasing range of which can easily be adjusted. We emphasize here the particular part played by the cholesteric liquid crystal-glass interface in the laser action of the fiber.

PACS. 42.55.Wd Fiber lasers – 42.70.Df Liquid crystals

1 Introduction

Rare-earth-doped fiber lasers are now commonly used in telecommunication devices and are of interest in the fields of medicine, sensing and spectroscopy. These applications require rugged, and as possible, low cost designs. The first Nd^{3+}-doped silica fiber laser demonstrated by Stone and Burrus was an end-pumped Fabry-Perot resonator in which the bulk mirrors were mounted directly against the fiber ends [1]. However, a number of disadvantages still remains with such a configuration: mechanical instability of the laser and excess cavity losses at the interface between the mirror and the fiber end due to impurities, fiber end cleaving quality, tilt and bending of the fiber, etc. [2]. Several improvements have been made to overcome these drawbacks, in form of loop reflectors [3], direct coated dielectric mirrors [4] or integrated Bragg grating reflectors [5]. They offer the potential to reduce the intracavity losses, nevertheless the wavelength of emission of these laser designs is, for a given fiber, restricted to a narrow band and the technology necessary to write Bragg gratings remains expensive.

The development of liquid-crystal-optical-components (LCOC) began in the eighties in large-aperture solid-state laser systems. These anisotropic fluids revealed to be a profitable alternative to conventional optical devices and furthermore gave birth to entirely new optical systems. The major characteristics of LCOC are: good optical quality at large apertures, high contrast, high transmission for passed polarization, high laser-damage resistance and low cost compared with this one of conventional optical devices [6]. Even though considerable care must be devoted to the fabrication of large aperture and high laser-damage threshold LCOC, to design narrow aperture and low power optical components based on liquid crystal optics is quite easy. This is particularly true in the case of devices including optic fibers such as this one presented in this work. Besides these qualities, there is nevertheless the highly scattering nature of the liquid crystal that should be taken into account while designing an optical component: it is necessary to reduce the associated losses. In a recent paper, Chang *et al.* have demonstrated a short pulse generation in a mode-locked fiber-laser using a cholesteric liquid crystal mirror [7]. In their set-up the CLC acts as a circularly polarizing mirror to induce passive mode-locking mechanism and suppresses the spatial hole burning inherent of a Fabry-Perot cavity.

In this paper we report some preliminary experiments on the feasibility of a Nd^{3+}-laser involving both the optical fiber and liquid crystal technologies. The investigated laser-cavity configuration is consisting of a Cholesteric Liquid Crystal (CLC) mirror butting the input end of a Nd^{3+} doped silica fiber. The helical axis of the mirror is parallel to the fiber, *i.e.* parallel to the light propagation direction and as a result, this light experiences a selective reflection provided that its wavelength is within a right spectral range which depends on the pitch of the cholesteric. Conversely, with such a resonator design, it should be possible to change in situ the wavelength region of the laser light emission by varying the physical parameters of the CLC mixture, namely the temperature or the thickness of the liquid crystal film.

[a] e-mail: pierre.carette@univ-artois.fr

2 Design of the CLC mirror

2.1 Optical properties of liquid crystals

Nematic liquid crystals are the basic materials of the LCOC. They are mostly constituted by elongated molecules with planar and rigid nuclei of two or more various rings and they can be schemed by the following structure:

$$R_1\text{- - -}X_1\text{- - -}A_1\text{- - -X- - -}A_2\text{- - -}X_2\text{- - -}R_2$$

where A_1 and A_2 are aromatic groups (which may be benzene, phenyl, cyclohexyl, biphenyl or pyrimidine rings or groups of rings), R_1 and R_2 are terminating aliphatic groups. The rings or groups of rings may be linked together or to the aliphatic chains directly or by groups X_1, X and X_2 of the types COO- (esters), -N=N- (azo compounds), -N=(O)- (azoxy compounds) or -CH=N- (Schiff bases).

In the nematic phase, locally, the long axis of the molecules fluctuates around a specific direction, which is represented by a vector field, called the director **n**. The material is optically uniaxial, the optical axis being coincident with the director. For most nematics, the optical birefringence is positive. In an ideal nematic phase, the director field is a constant one. In case of chiral molecules, one obtains phases for which the director field experiences a twisted configuration: the director is normal to an helical axis and rotates along with it.

Because many chiral nematic liquid crystals are composed of cholesteryl derivatives, they are often referred as cholesterics. These cholesterics are optically characterized not only by the ordinary and extraordinary indices, but also by the pitch, p, of the helical structure. Moreover the cholesterics are optically active, that is, they rotate the direction of linearly polarized light. By adding percentage amounts of cholesteric twisting agents to ordinary nematics, it is possible to create a left-handed or a right-handed twist in the resulting cholesteric mixtures, with any pitch value.

An other interesting feature of these materials is the selective reflection. It is obtained when optical radiation propagating along the cholesteric helix is located within a narrow band $\Delta\lambda_B$ centered on the Bragg wavelength λ_B which satisfies the condition:

$$\lambda_B = 2n_{av}\Lambda = n_{av}p, \tag{1}$$

where n_{av} is the average refractive index of the cholesteric medium and $\Lambda = p/2$ the pitch of the material. An incident light with a wavelength λ lying in this band will interact with the cholesteric depending on its polarization state. In such an helical structure it is convenient to split the incident optical radiation into left and right-handed circularly polarized components. The component whose handedness is opposite to that of the structure will pass the material, the other component being reflected (Fig. 1a). All other wavelengths will pass through the helical structure without interacting (Fig. 1b).

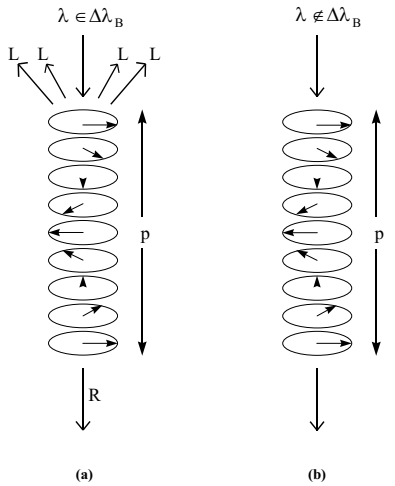

Fig. 1. Selective reflection effect in a left-handed cholesteric structure for unpolarized light: (a) $\lambda \in \Delta\lambda_B$, the left-handed circularly polarized portion of the light (L) is reflected and the right-handed one (R) is transmitted, (b) $\lambda \notin \Delta\lambda_B$, no interaction of the light with the cholesteric structure.

2.2 Experimental

In practice, because of the existence of various sources of defects the spontaneous molecular order (*i.e.* the helical structure) within the bulk of a CLC does not extend beyond some thousands of ängstroms. Increase of this distance over tens of micrometers can be achieved by creating a preferred direction of the liquid crystal at the fluid-cell interface. Anchoring of liquid crystal molecules in the homogeneous configuration is carried out by unidirectionally rubbing the bare glass inner surface of the cell with a fine polishing (0.1-μm) diamond compound. An homogeneous alignment may be obtained too with unidirectional buffing of a thin polymer layer deposited by spin coating. Test samples of the CLC mirror are prepared in which the CLC is sandwiched between two surface treated microscope slides maintained parallel by Mylar spacers.

2.3 Results

A key to achieve a liquid crystal mirror for laser cavity purpose is the control of the selective reflection band of the liquid crystal, say to adjust the pitch of the cholesteric medium to satisfy the Bragg condition for the wavelength of the desired laser oscillation.

A theoretical expression of the reflectivity R of a CLC layer of thickness d is given by [8]:

$$R = \frac{1}{1 + \dfrac{1-(\nu/\kappa)^2}{\sinh^2\left[\kappa d\sqrt{1-(\nu/\kappa)^2}\right]}}, \tag{2}$$

where κ is the coupling coefficient $n_m(\omega/c)$ and ν the detuning parameter $2\pi n_{av}(1/\lambda - 1/\lambda_B)$. The average index

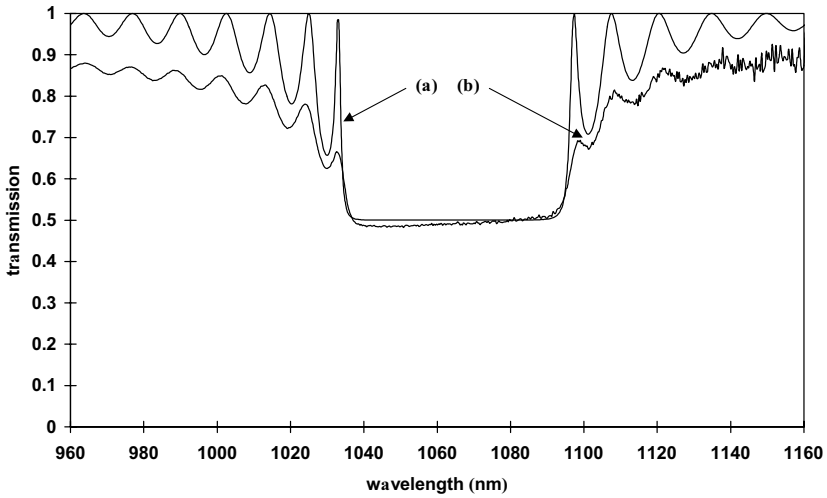

Fig. 2. Transmission spectrum of the used cholesteric liquid crystal mirror ($T = 22\,^{\circ}$C): (a) calculated, (b) experimental.

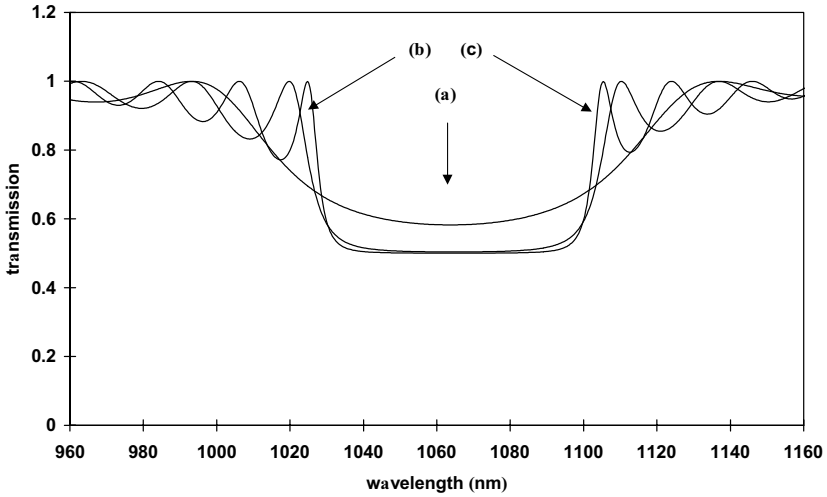

Fig. 3. Calculated transmission spectrum of the used CLC mixture for unpolarized incident light and for a varying fluid thickness d: (a) $d = 5$ μm, (b) $d = 10$ μm, (c) $d = 15$ μm.

$n_{\rm av}$ and n_m are connected to the optical dielectric constants of the CLC $\varepsilon_{\parallel}$ and $\varepsilon_{\perp}$ respectively parallel and perpendicular to the director by the relations:

$$n_{\rm av} = \sqrt{(\varepsilon_{\parallel} + \varepsilon_{\perp})/2}, \tag{3}$$

$$\text{and} \quad n_m = |\varepsilon_{\parallel} - \varepsilon_{\perp}|/4\sqrt{(\varepsilon_{\parallel} + \varepsilon_{\perp})/2}. \tag{4}$$

The target value of the selective reflection band center was 1064 nm which is the mean wavelength of the $^4F_{3/2} \rightarrow {}^4I_{11/2}$ laser transition of Nd^{3+}. The used liquid crystal is a left-handed mixture of cholesterol nonaoate (28%), cholesterol myristate (9%) and nematic liquid crystal (ZLI 1083 from Merck; 63%). Such a mixture has its clearing point at 52 °C. The weight percentages of the mixture have been empirically adjusted to peak the reflectivity to the target value in checking the transmission spectra of planary aligned samples using a 0.5 m Acton Research corporation triple grating monochromator (model Spectra Pro 500), equiped with a Reticon Optical Multichannel Analyzer (OMA), model 1453A. The obtained selective reflection band is centered at 1066 nm at room temperature of 22 °C and the characteristics of the used liquid crystals mixture derived from fitting of experimental transmission curves for calibrated slab thickness of 5.9, 12 and 18 μm are: $n_{\rm av}$= 1.766, n_m= 0.0525 and $p = 0.604$ μm. Although these values are of rather poor accuracy, they are sufficient to determine the thickness of the liquid crystal layer which is necessary to reach a 100% reflectivity for the left-handed circular light polarization. The experimental transmission spectrum of the CLC mirror between 960 nm and 1160 nm is presented in Figure 2 where a comparison is made with the calculated transmission curve obtained using equation (2) and the experimental parameters given above. The thickness of the cholesteric medium is 28 μm. The transmission rate within the selective reflection band is 50% as expected for unpolarized light provided that the thickness of the cholesteric medium exceeds 15 μm as shown in Figure 3 where theoretical transmission curves are drawn for various slab thicknesses. In the pump

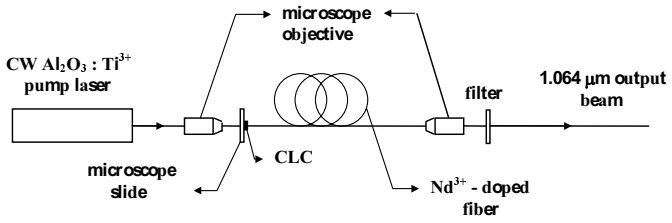

Fig. 4. Experimental setup.

wavelength region around 800 nm, the transmission of the CLC is found to be 90% for polarized or unpolarized light. No significant power absorption is observed in the CLC at both pump and fiber laser wavelengths.

The transmission spectra have been recorded at different temperatures, say 20, 25, 30, 35 and 40 °C, in order to evaluate the temperature drift of the selective reflection band of the CLC mirror. The mean temperature shift is 3.5 nm K^{-1}. The selective reflection band is shifted towards longer wavelengths as the temperature increases.

3 Application to a Nd^{3+} fiber laser

Fiber laser cavities are usually closed by a mirror or a photowritten Bragg grating with a high reflectivity coefficient and an output coupler with a low reflectivity coefficient. We have realized a Nd^{3+} fiber laser using a CLC mirror as high reflectivity mirror and the bare fiber end as output coupler. The laser action of this resonator (configuration b) has been investigated as compared to the behavior of the same fiber laser without any CLC coupler (configuration a).

3.1 Experimental

The used experimental setup is shown in Figure 4. Basically, a pump laser excites a rare earth doped fiber, either a bare one (configuration a) or bounded at one end with a CLC layer (configuration b). The pump source is an Ar^+ Coherent Radiation model Innova 310 laser pumped Ti:sapphire laser Coherent Radiation model 899-01 operating at 803.5 nm. The pump beam is focused into the fiber core using a long working distance microscope objective (×50) which transmits 63% of the pump energy. The light emerging out of the system is analyzed using a 0.5 m Acton Research Corporation triple grating monochromator model Spectra Pro 500, equiped with a Reticon Optical Multichannel Analyzer (OMA) model 1453A.

The fiber used as amplifying medium is a single mode, 2.7 m long fiber model FPGA 519 Nd manufactured by the Centre National d'Études et Telecommunications (CNET) laboratory in Lannion, France, core codoped with germanium, aluminium, and 330 parts in 10^6 Nd^{3+} ions (3×10^{24} ions/m^3). The cladding dopants are fluoride and phosphorous, the core diameter is 1.8 μm and the cut off wavelength is 790 nm. The CLC is sandwiched between the input end of the fiber and a microscope slide.

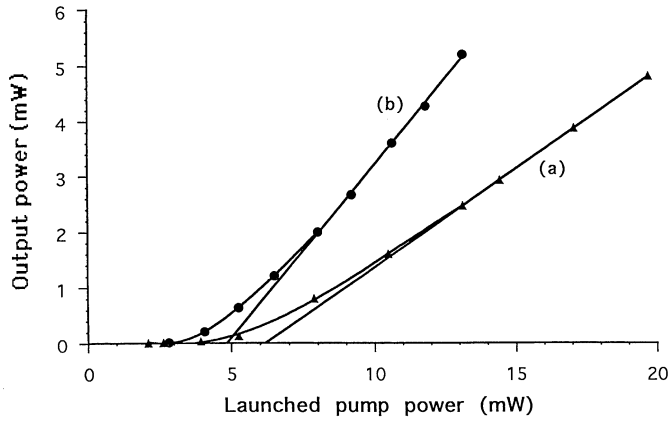

Fig. 5. Characteristic laser curves for the doped fiber with (•) and without (▲) a CLC mirror.

The surface of this slide has been treated to achieve a planar orientation of the CLC and the distance between the slide and the fiber can be adjusted by means of a piezoelectric stepper (0.1 μm step) to a thickness slightly above the thickness just necessary to obtain a saturation of the reflectivity at 1064 nm in order not to jeopardize the thermal stability of reflectivity, say 20 μm. In such a configuration, the helical axis is parallel to the fiber axis, *i.e.* to the beam propagation.

3.2 Results and discussion

We have measured the launched pump power and the output power in both configurations a and b. The derived laser characteristic curves are collected in Figure 5. In case of a mirrorless laser, the curve is non linear below a 13 mW pump power: this is connected to the fact that the optical feedback is provided only by the Fresnel reflections from the fiber ends which are only 3.5%. Such a non linear behavior is comparable to that one of a Nd^{3+} doped fiber superluminescent source (SLS) [9]. For high pump powers, the number of roundtrips undergone by the lightwave inside the amplifying medium is large and the resonator becomes a classic laser oscillator. Thus, above a 13 mW launched pump power, the characteristic curve is practically linear and the slope efficiency is found to be 35.5%. As the reflectivity of the output coupler is very low, in case of low pump power the guided spontaneous emission is mostly transmitted by the fiber output end. So there is no classical laser threshold for this type of resonator. However we can define an extrapolated threshold using the linear part of the characteristic curve for high launched pump power values. An extrapolated threshold of 6.2 mW is then found.

In the configuration b, with a CLC mirror butting the input fiber end, the characteristic curve shows the same nonlinear behavior, however this feature occurs for lower pump powers and, in addition, the efficiency is increased. Both these features can be ascribed to the reflectivity enhancement of the input mirror and to its wavelength selectivity. The improved slope efficiency is 62.1% and the

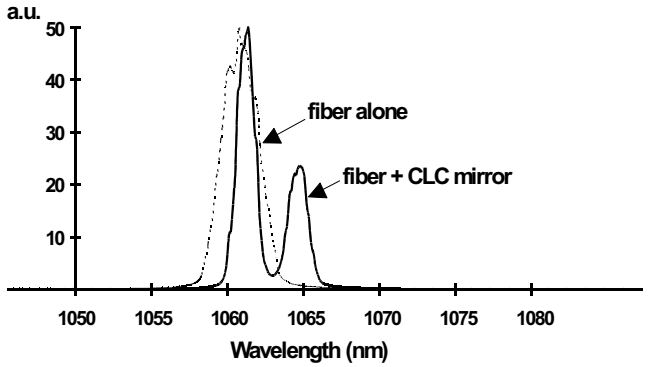

Fig. 6. Comparison of the emission spectra of the laser obtained with and without a CLC mirror.

extrapolated threshold is 4.8 mW. The obtained spectrum is shown in Figure 6 together with this one of the previous resonator configuration. Two main features are observed in these spectra: first, a line narrowing of the 1061 nm line and second, appearance of an extra line at 1064 nm. The polarization features exhibited by these lines will be ascribed below to the essential part played by the CLC-glass interface on the laser action.

A theoretical model of the laser action based on the photon flow conservation law in a cavity [10] allows to calculate the theoretical slope efficiency of a doped fiber laser as a function of the reflectivities R_1 and R_2 of the mirrors. In this model, the signal power through the output coupler P_S is given by the following simplified formula:

$$P_S = \frac{(\lambda_P/\lambda_S)}{1+(1-R_1)(1-R_2)\sqrt{R_2/R_1}}(P_P - P_{th}) \qquad (5)$$

where λ_P and λ_S are the pump and signal wavelengths P_P the launched pump power and P_{th} the threshold power. In the case of a Nd^{3+} four levels laser the signal wavelength of the $^4F_{5/2} \rightarrow {}^4I_{11/2}$ transition λ_S is 1064 nm and the pump wavelength of the $^4F_{5/2},\ ^2H_{9/2} \leftarrow {}^4I_{9/2}$ transition is 803 nm. The derived theoretical laser efficiencies for $R_1 = R_2 = 0.035$ and for $R_1 = 0.5$ and $R_2 = 0.035$ are respectively 37.7% and 66.4% in good agreement with our experimental results.

The polarization of the laser emission of a fiber laser depends partly on the cross-sectional anisotropy of the active ions within the fiber core [11] and on the polarization induced by any polarization sensitive element. The experimentally observed polarization of the laser emission is elliptic when it acts without a CLC mirror as it may be expected from a laser utilizing a fiber supporting two orthogonal linear polarization modes. Setting up a CLC mirror as high reflectivity coupler on the input end of the same Nd^{3+} fiber makes the laser emission practically linearly polarized. This behavior may seem at first sight somewhat paradoxical as the polarization of the light reflected by a CLC mirror is supposed to be circularly polarized. In fact, this statement is true assuming that the refraction index of the outside medium is very close to the mean index of the cholesteric medium. We have therefore to consider the actual polarization of the light that is completely reflected by the CLC mirror. Let us suppose that the CLC coupler has a maximum reflectivity. This problem has been treated extensively by Good and Karali in the case of a light propagation parallel to the axis of the helical cholesteric structure [12]. The dielectric tensor within the crystal is assumed, as in the usual way, to have the elements:

$$\begin{aligned} \varepsilon_{xx} &= \varepsilon_{av}(1+\delta\cos 2q_0 z), \\ \varepsilon_{yy} &= \varepsilon_{av}(1-\delta\cos 2q_0 z), \\ \varepsilon_{xy} &= \varepsilon_{yx} = \varepsilon_{av}\delta\sin 2q_0 z, \end{aligned} \qquad (6)$$

where $q_0 = 2\pi/p$ and $\delta = \varepsilon_m/\varepsilon_{av}$ with $\varepsilon_m = |\varepsilon_\parallel - \varepsilon_\perp|/2$. It is straightforward to show that wave equations for light propagation along the helical axis z have the form:

$$\partial^2 E_x/\partial z^2 = 1/c^2(\varepsilon_{xx}\partial^2 E_x/\partial t^2 + \varepsilon_{xy}\partial^2 E_y/\partial t^2)$$

and

$$\partial^2 E_y/\partial z^2 = 1/c^2(\varepsilon_{xy}\partial^2 E_x/\partial t^2 + \varepsilon_{yy}\partial^2 E_y/\partial t^2), \qquad (7)$$

where c is the speed of light in vacuum. Equations (7) can be solved more conveniently in terms of the components

$$E^\pm = E_x \pm \mathrm{i}E_y = \sum_{j=1}^{4} A_j^\pm \exp\left[\mathrm{i}(\ell_j \pm 1)q_0 z\right], \qquad (8)$$

where $\ell_j^2 = y + 1 \pm (4y + \delta^2 y^2)^{1/2}$, $y = (k_0/q_0)^2\varepsilon_m$, with $\ell_1^2 > \ell_2^2$ and $\ell_3 = -\ell_1,\ \ell_4 = -\ell_2$. The selective reflection band corresponds to values of k_0 for which $\ell_2^2 < 0$. Transmission within the selective reflection band for a thick slab of thickness d can be treated in the case of a left-handed crystal disregarding all but the terms proportional to $\exp(\mathrm{i}\ell_2 q_0 d)$. The polarization rate of the incident wave that is completely reflected by the cholesteric medium, defined by $\chi = E_y/E_x$ is shown by Good and Karali to be:

$$\chi = \mathrm{i}\left[\beta(1+\ell_2\rho_2) - \mathrm{i}\rho_2\right] / \left[1 + \mathrm{i}\beta(\ell_2 - \rho_2)\right], \qquad (9)$$

where $\beta = n_1 p/\lambda$, n_1 is the index of the medium outside the cholesteric, $\rho_2 = 2\ell_2/(\ell_2^2 + 1 - y + \delta y)$ and λ is the wavelength of the radiation. The x-axis is chosen to coincide with the direction of the liquid crystal director on the input surface of the cholesteric medium. χ describes the polarization of the beam: if χ is $+\mathrm{i}$ $(-\mathrm{i})$, the light is right-hand (left-hand) circularly polarized; if χ is real, the light is linearly polarized; otherwise, it is elliptically polarized. Figure 7 shows a plot of real and imaginary parts of the polarization rate of the wave that is completely reflected in the case of the used left-handed cholesteric mixture for which $\varepsilon_{av} = 3.12$ and $\varepsilon_m = 0.18$. Various values of the wavelength (in nm) are considered as indicated in the scheme. This representation clearly shows that the glass medium of index $n_1 = 1.4756$ of the fiber causes an elliptic polarization of the light of the reflected beam. The polarization of the reflected light can be entirely characterized by the angle of tilt Ψ between the axes $O\zeta$ and

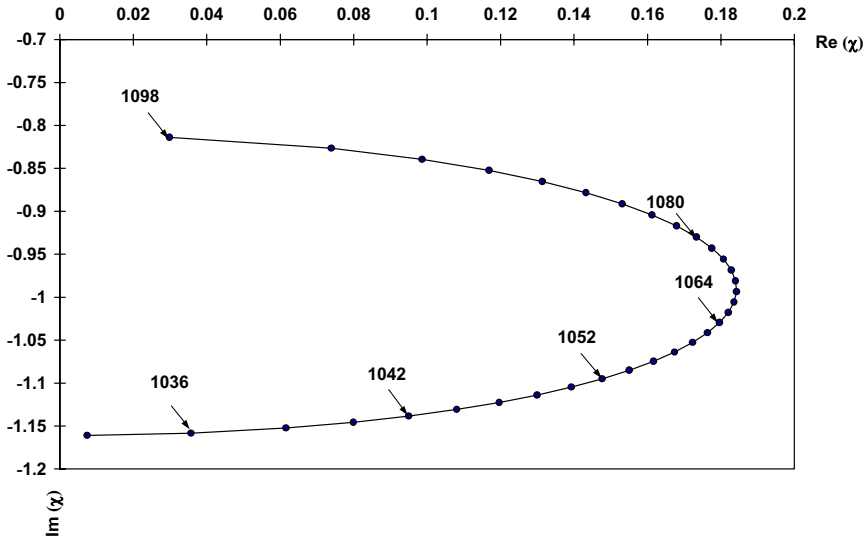

Fig. 7. Real and imaginary parts of the polarization rate of the wave that is completely reflected by the used CLC mirror.

Oη of the elliptical vibration and the Ox and Oy directions and by $\tan\varphi = E_{\eta m}/E_{\zeta m}$ where $E_{\zeta m}$ and $E_{\eta m}$ are the amplitudes of the electric field in the Oζ and Oη directions. If one represents this elliptically polarized light impinging the cholesteric medium at $z = 0$ in the sense of $z > 0$ by the incoming field

$$\mathbf{E}_{\rm inc}(z=0) = E_{xm}\cos(\omega t)\mathbf{e}_x + E_{ym}\cos(\omega t+\gamma)\mathbf{e}_y, \tag{10}$$

where E_{xm} and E_{ym} are the amplitudes of $\mathbf{E}_{\rm inc}$ in the directions defined by the rectangular unit vectors $\mathbf{e}_x$ and $\mathbf{e}_y$ and where γ is the phase shift between the components E_x and E_y of $\mathbf{E}_{\rm inc}$, one gets [13]

$$\tan 2\Psi = (\tan 2\alpha)\cos\gamma, \tag{11}$$

with $\tan 2\alpha = E_{ym}/E_{xm} = \sqrt{\Re^2(\chi)+\Im^2(\chi)}$ and $\tan\gamma = \Im(\chi)/\Re(\chi)$, where $\Re(\chi)$ and $\Im(\chi)$ are the real and imaginary parts of χ. A straightforward calculation allows us to derive that

$$\tan\varphi = \frac{\left[1+\chi^2-\sqrt{(1+\chi^2)^2-4\Im^2(\chi)}\right]^{1/2}}{\left[1+\chi^2+\sqrt{(1+\chi^2)^2-4\Im^2(\chi)}\right]^{1/2}}. \tag{12}$$

The main polarization characteristics of the totally reflected beam are collected in Table 1 for both the wavelengths $\lambda_1 = 1061$ nm and $\lambda_2 = 1064$ nm of the laser.

In order to determine how the properties of the CLC mirror affect the fiber laser operation we have to consider the birefringence of the fiber which is characterized by two slightly different indices of refraction n_{1X} and n_{1Y} for two linearly polarized radiations in the rectangular directions OX and OY perpendicular to the Oz axis. Let u be the angle between the axes Oζ and Oη of the elliptically polarized light at $z = 0$ and the birefringence directions OX and OY of the fiber (Fig. 8). Using again equation (11) in the reference frame OXY of the fiber, one can write

$$\tan 2u = (\tan 2\theta)\cos\gamma', \tag{13}$$

where γ' is the phase shift between the components E_X and E_Y of $\mathbf{E}_{\rm inc}$.

At least it is easy to establish that

$$\cos 2\theta = (\cos 2u)\cos 2\varphi. \tag{14}$$

Let us now consider, within the fiber, the left-handed polarized elliptical light that will be totally reflected by the

Table 1. Calculated polarization characteristics of the laser radiations λ_1 and λ_2.

λ (nm)	1061	1064
γ (°)	279.3	279.9
Ψ (°)	55.9	52.2
φ (°)	40	40
α (°)	46.3	46.8

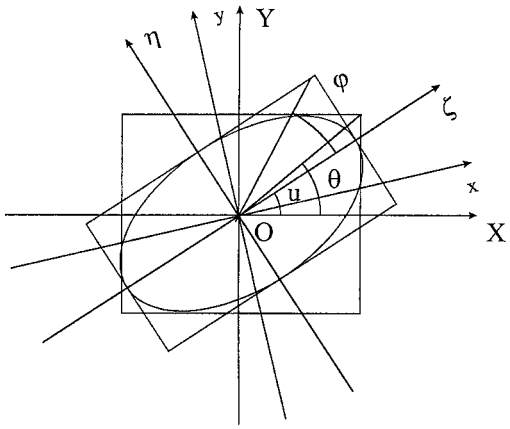

Fig. 8. Tilt of the major axis of the left-handed elliptically polarized radiation on the fast axis of birefringence of the fiber.

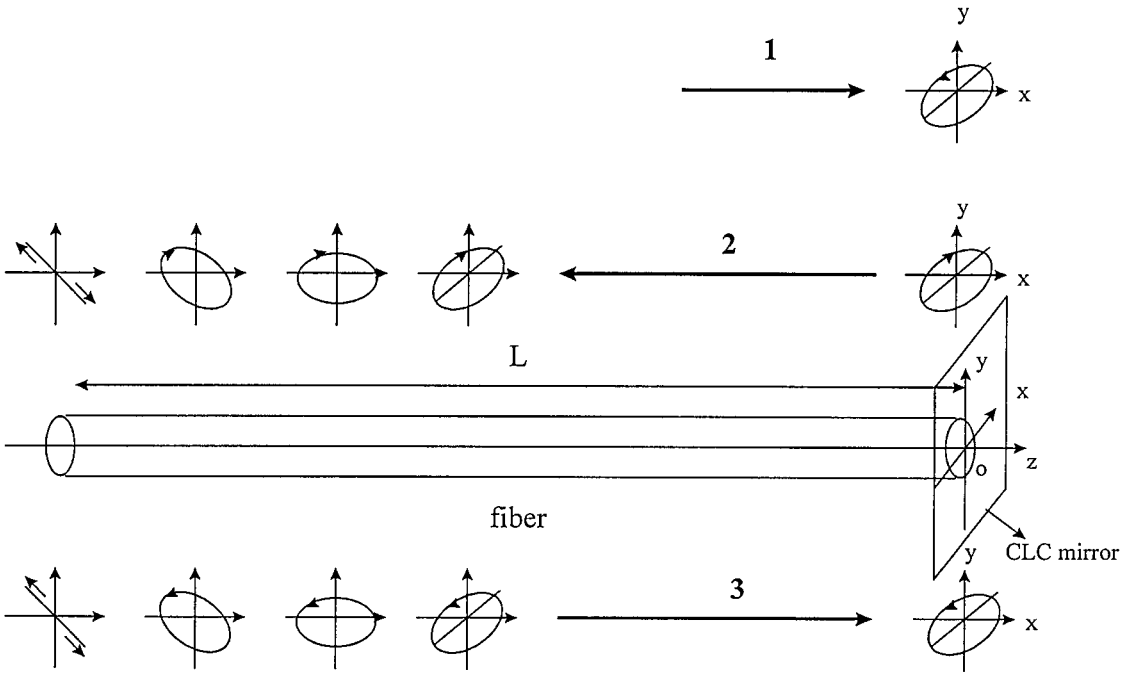

Fig. 9. Illustrating the light polarization required on the output end for laser action in the fiber. Waves 1 and 3 must have the same elliptical characteristics which are imposed by the CLC mirror. Wave 2 which experiences a 100% reflection on the CLC mirror keeps its initial handedness. This handedness is periodically changed during the wave propagation toward the output end of the fiber by the anisotropy of the core. The dielectric reflection on the output interface changes the handedness of the elliptical polarization so that it is necessary to get a linear polarization on this surface to obtain a wave identical to wave 1 on the CLC mirror surface. Notice that the various ellipses in the drawing are viewed by an external observer placed in front of the CLC mirror.

CLC mirror and propagating toward this high reflectivity coupler in the sense of $z > 0$. This wave is labelled as wave 1 in Figure 9. When this left-handed elliptically polarized light is incident upon the CLC mirror, the reflected field preserves its original handedness (wave 2 in Fig. 9) and can be written as

$$\mathbf{E}_{\text{ref}}(z) = E_X \cos[\omega t - \gamma_1(z)]\mathbf{e}_X - E_Y \cos[\omega t - \gamma_1(z) - \Delta\gamma_1(z) + \gamma']\mathbf{e}_Y, \quad (15)$$

where $\gamma_1(z) = 2\pi n_{1X}|z|/\lambda$ and $\Delta\gamma_1(z) = 2\pi(n_{1Y} - n_{1X})|z|/\lambda$ is the phase shift due to the birefringence of the fiber.

When this reflected wave reaches the end of the fiber at $z = -L$, it undergoes a second reflection at the glass-air interface and experiences a 180° phase shift as a result of a direction change from the $-z$ to z-axis. It is clear, as shown in Figure 9 that the wave labelled as wave 3 after a round trip in the cavity recovers exactly the polarization characteristics of wave 1 provided that the polarization on the output coupler is linear. This condition is achieved every time that $\gamma' - \Delta\gamma_1(-L) = m\pi$ with m integer, *i.e.* for a wavelength for which the phase shift due to the CLC mirror is compensated by the anisotropy of the fiber core. The corresponding linear polarisation directions in the plane of the output coupler are then tilted by the angle $\upsilon = \theta_1 - \theta_2$ where θ_1 and θ_2 are the values of the angles of tilt on the OX direction of the linearly polarized radiations at the fiber end for the two observed laser lines λ_1 and λ_2 (Fig. 10). Each angle θ can vary within a range extending from 40° to 45° as a function of u as shown in Figure 11. Therefore, the angle υ between the two linearly polarized modes can vary from 80° to 90° in good agreement with the experimental observation.

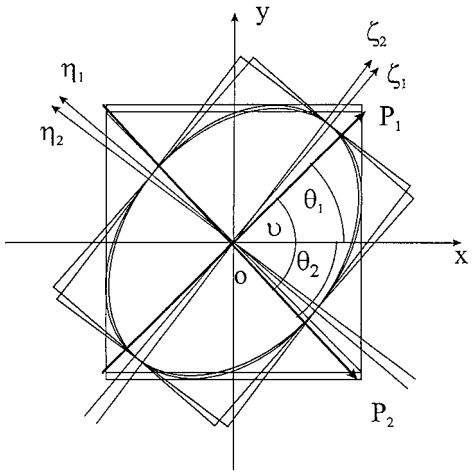

Fig. 10. Directions of polarizations OP_1 and OP_2 of the laser lines in connexion with the two elliptically polarized waves that are 100% reflected by the CLC mirror.

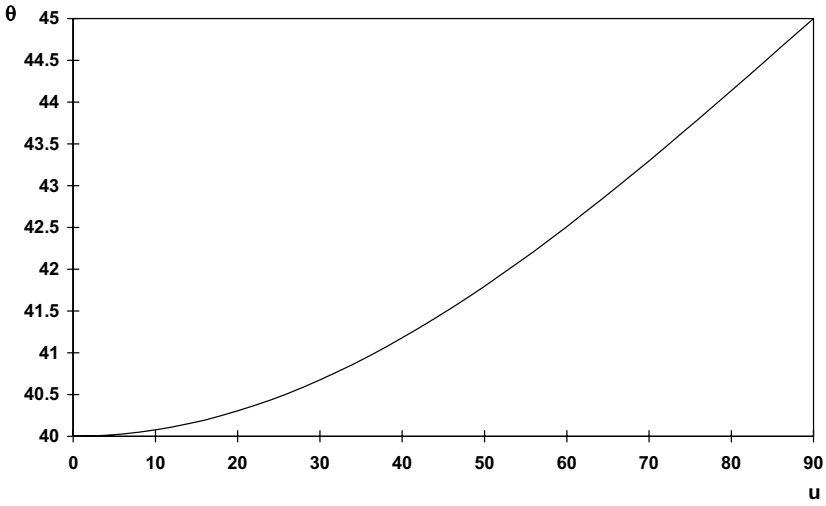

Fig. 11. Variation of the angle of tilt θ (°) of a linearly polarized mode of the laser on the direction of the OX axis of birefringence of the fiber as a function of the angle u (°) formed by this axis and the major axis of the elliptically left-handed polarized light wave at the fiber-cholesteric interface.

4 Conclusion

We have demonstrated for a room-temperature CW Nd^{3+}-doped fiber laser around 1.06 μm using a CLC mirror. A resonator, the optical feedback of which is due to the 3.5% Fresnel reflections from the fiber ends, was also investigated in comparison with the incorporated CLC mirror resonator. In the case of the CLC mirror cavity, an obvious enhancement of the laser action has been observed with a 62.1% slope efficiency with a 4.8 mW extrapolated threshold. The performances of this device are comparable with those of more usual set-ups. A study of the characteristics of the CLC mirror has shown the part played by the glass-cholesteric medium interface on the fiber laser operation. A substantial gap between the values of the mean index of the cholesteric medium and the index of the fiber core results in well defined elliptical polarization characteristics of the wave entirely reflected by the high reflectivity coupler. The limit conditions for the travelling wave on the surface of the output end of the fiber demand that the laser radiation is linearly polarized as it is experimentally observed.

The success in obtaining a laser action with a CLC mirror cavity, with no limitation due to mirror damage for powers up to 200 mW, suggests that CLC may be used as good optical components in association with an optical fiber provided that this prototype of laser resonator might be improved by enclosing the CLC at the fiber ends. Nevertheless this work should be regarded as a test-bench for the use of a cholesteric medium, independently of its nature, as a cavity mirror in a doped fiber-laser.

The Laboratoire de Chimie des Interfaces et Applications participates to the Centre d'Études et de Recherches Lasers et Applications, supported by the Ministère chargé de la Recherche, the Région Nord/Pas de Calais and the Fonds Européen de Développement Économique des Régions. It participates to the Groupe de Recherches du CNRS No. 606.

References

1. J. Stone, C.A. Burrus, Appl. Phys. Lett. **23**, 388 (1973).
2. P. Urquart, in *Rare Earth Doped Fiber Lasers and Amplifiers*, edited by M.J.F. Digonnet (Marcel Decker, New York, 1993).
3. I.D. Miller, D.B. Mortimore, P. Urquart, B.J. Ainslie, S.P. Craig, C.A. Millar, D.B. Payne, Appl. Opt. **26**, 2197 (1987).
4. M. Shimitzu, H. Suda, M. Horiguchi, Electron. Lett. **23**, 768 (1987).
5. I.M. Jauncey, L. Reekie, R.J. Mears, D.N. Payne, C.J. Rowe, D.C.J. Reid, I. Bennion, C. Edge, Electron. Lett. **22**, 987 (1986).
6. S.D. Jacobs, K.A. Cerquia, K.L. Marshall, A. Schmid, M.J. Guardalben, K.J. Skerrett, J. Opt. Soc. Am. B **9**, 1962 (1988).
7. D.I. Chang, H.Y. Kim, M.Y. Jeon, H.K. Lee, D.S. Lim, K.H. Kim, I. Kim, S.T. Kim, Opt. Commun. **162**, 251 (1999).
8. J.C. Lee, S.D. Jacobs, J. Appl. Phys. **68**, 6523 (1990).
9. K. Liu, M. Digonnet, H.J. Shaw, B.J. Ainslie, S.P. Craig, Electron. Lett. **23**, 1320 (1987).
10. T. Georges, E. Delevaque, Opt. Lett. **16**, 1113 (1992).
11. R. Leners, G. Stéphan, Quant. Semiclass. Opt. **7**, 757 (1995).
12. R.H. Good, A. Karali, J. Opt. Soc. Am. A **23**, 2145 (1994).
13. M. Born, E. Wolf, in *Princiles of Optics* (Pergamon Press, 1986).